LUPINE PUBLISHERS

An archive of organic and inorganic chemical sciences

DOI: 10.32474/AOICS.2021.05.000209

ISSN: 2637-4609

Research Article

Biofuels at Optimal Condition of Ignition in A 100 Kwe MGT and Their Nox Emissions Paths

Vincenza Liguori*

Università degli Studi di Napoli Federico II

***Corresponding author:** Vincenza Liguori, Università degli Studi di Napoli Federico II

Received: April 24, 2021 **Published:** June 7, 2021

Abstract

In the annular burner of a 100 kWe micro gas turbine (MGT), combustion begins or is supported by pilot. flames appropriately located. These can be thought as partially stirred reactors in which reagents are considered immiscible at the molecular level and homogeneous in the spatial dimension. The survey reports of a numerical sensitivity analysis developed in two steps. The first on the pilot flame model, focusing on some of the most well-known kinetic schemas of hydrocarbon combustion simulation, has helped to extrapolate the optimal conditions of ignition. Performances of different gaseous biofuels, simulated via the kinetic model's methane 17, methane 30, and GRI Mech 3.0, to extrapolate, in a sort of principal component analysis to compute NOx production. Operational environment described by the fluid- dynamic parameter MIXT, that identifies the partially stirred conditions of the flame; temperature at ignition, Tinit; the best feeding ratio. GRI Mech 3.0 is the only model able to calculate NOx production and so it was considered at the optimal conditions, by induction, in a sort of extensive meta-analysis.

Keywords: NOx; GRI Mech 3.0; 100 kWe MGT; Monte Carlo model; adaptive chemistry Biofuels

Introduction

The micro gas turbines (MGTs) [1,2] are energy and mechanical devices still considered as technologically young. These devices have been developed since the late 1940s in the aircraft industry and were then borrowed (since the 1990s) by manufacturing sectors as stationary systems for electricity production. They are available in a wide range of rated power outputs, i.e., from 5 to 250 kW. Designed to work with natural gas, their good performance is assured by a set of combined effects. Climate and geographical position are external conditions that affect the thermodynamic cycle, while. the structure and technology of the burner, the established chemical and physical conditions, and the supplied fuels are the internal variables. The evolution of combustion methodologies and techniques [3,4] best suitable for the burner of the micro gas turbine [5-7] was investigated in the different related topics: turbulence [8], fluid dynamics, the mathematical models, kinetics, and emissions. These various fields of investigation are often interconnected [9]. From the evaluation of the best fitting numerical model [10] of combustion in the turbulence range to the production of energy by means of coupled devices, measuring the cogeneration combined heat power (CHP) between MGTs and natural gas-fueled internal combustion engines and, e.g., also characterizing their emissions [11]; other investigations points are related to the most fitting thermodynamic cycle if devices fed with renewables, e.g., about the organic Rankine cycle (ORC), and its performance in the MGT[12]. Furthermore, the studies on their thermoacoustic instabilities [13]. The study [14]., records of the ignition conditions at the pilot flame; the latter, is modeled as a partially stirred reactor (PaSR); the numerical comparison is extrapolated from the outcomes of the evolution of the simulation of some well-known kinetic models. Those applied were as follows: methane 17 [15], methane 30 [16], and GRI Mech 3.0 [4]. These kinetic models have an increasing degree of complexity and completeness. They are correlated with each other in terms of chemical species since they all evaluate gas-phase hydrocarbon combustion reactions. Among them only GRI Mech 3.0 explains the development of NOx combustion and so it is helpful for the second part of the investigation that is focused on the extrapolation of some common species connecting all the schemas, also linked to NOx production species. The ambitious objective is to produce an autonomous and shorter computational model of NOx evolution, proceeding almost in contrast to the adaptive chemistry approach, [17], that addresses this issue by replacing the full mechanism with an entire library of locally accurate, reduced kinetic models. The pilot flame of the MGT, which starts or reinforces combustion, is reproduced by the PaSR model by means

of a system of ordinary differential equation (ODE) equations. The existing computational fluid dynamics (CFD) algorithms are very intensive in terms of computational cost, and they scale up with the number of chemical species modeled; if N is the number of species, then the CPU demand is N^2 or N^3 [18,19].

The CPU time and memory overheads, which are required to solve reactive flows with detailed kinetics, are alleviated by two main classes of methods. These include model simplification and model reduction. The first method trims any non-important species and reactions from the detailed mechanism, while the second method produces a small number of global reaction steps, of which the rates are computed based on the elementary rates. They are usually in a series. The survey proposed searches for a sort of model simplification by modifying the detailed kinetics. The problem consists of determining the trajectory of the vector x(t), analytically or numerically integrating the system of equations starting from an initial condition x (0). Obviously, increasing the number of species that take part in the reaction, the number of stages that make up the model, or the degree of nonlinearity of the equations increases the degree of complexity of the ODE system and therefore the difficulty in solving it [20]. Such problems are simplified by Monte Carlo theory [21,22], which naturally allows the sensitivity analysis. It was performed by the increasing and the decreasing of each value of each parameter describing the PaSR model, with respect to the assigned sampling values, in a multivariate approach [23,24,25]. The ignition condition has the main constraint in the fluid dynamic conditions. of partial stirring, but it is to be satisfied in lean feeding. The related NOx productions are highlighted to extrapolate a connection among the common reaction evolutions in which NOx involved from the different simulations, started from the different kinetic models. It can be useful to deduce a simplified and, to all the analyzed gaseous blends, a commonly valid NOx production path. The MGT, by design conditions, are very low NOx emissive. The NO production is widely previously investigated, e.g., in the interactions between them and hydrocarbon mixtures at low temperatures [26], also improving by the analysis of the same problem at high temperatures, specifying the main hydrocarbon intermediates produced and NOx reactions under reburning conditions [27]. The connection between kinetics and fluid dynamics on NOx production, at changing of sources, e.g., if the source is syngas [28,29]. Moreover, the evaluation of the related development at the changes of the operational parameters, such as at the influence of pressure and temperature on De-NOx processes [30]. For what conceive the reduction of the chemical manifolds, the different perspectives of investigations run by means of the computational singular perturbation CSP theory [18,31], reinforced by conclusions and approaches about the chemical states of the involved reactions [32,33,34]; and their further developments related to the implementation of simplified chemical kinetics based on low-dimensional manifolds [35,36,37,38]; by measuring the degree of interaction among the involved species [39]; or by using some other different mathematical tricks: e.g. by adopting a reaction matrix [40]. Many researchers are investigating how to reduce the calculation time of the GRI Mech 3.0 model by means of indirect approaches. On this line of research [41], have observed changes to the burning velocity of premixed flames for a mixture of CH4/H2, by supplying an air flow of modified composition, by replacing the CO_2 with N_2. But what is wanted in this analysis does not regard strictly GRI Mech 3.0 calculation time by using some tricks, as more as a sort of optimization on a focused path of its evolution.

It was focused on the role of NNH in the formation of NO, as a control phase to choose the schema of the reaction in chemical NOx developments [42]. The weight of computational cost from comparison between the GRI Mech 3.0 and the Lawrence Livermore n-heptane mechanisms via a reaction elimination was investigating, looking for the optimally reduced kinetic models by just eliminating the excess reactions and deleting the NOx developments [43]. In contrast, the peculiarity of our survey is the highlighting on the NOx formation reactions. The work proceeds with the help of the three kinetic models: methane 17; methane 30; GRI Mech 3.0. A subset of mechanisms reporting the common species in the minimum useful number to reproduce the nitrogen oxide reactions is extrapolated via of a sort of principal component analysis PCA [44], a refinement of the sensitivity analysis.

Material and Methods

Transport phenomena [45], turbulence, mixing and kinetics, [46,47], are the scientific areas related to the investigated problem. A pilot flame was significantly modeled by a Partially Stirred Reactor (PaSR), represented in [Figure 1]. It is a tool of the library of commercial software Chemin (from the User guide, 2003, the PaSR model); the version 3.7.1 was used for the simulations. By making some simplifying assumptions, the PaSR provided a phenomenological approach that shows the sensitivity of the reaction system to delayed micro-mixing. For instance, in a fuel-lean system, decreasing the mixing frequency had the effect of delaying combustion. That produced a greater range of local temperatures and local concentrations. The thermodynamic features (ranges of pressure, temperature, and fuel/air equivalence ratio of the supplied fuels) are presented in [Table 1]. For a flame considered as a system under homogenous spatial thermodynamic conditions with non-perfect molecular diffusion, the reactive species are considered immiscible at the molecular level and homogeneous in the spatial dimension. The mixing [48-50], conditions were expressed by means of an adaptation to the gas phase of the model, the so-called Curl's model [51,52], originally born for mixtures in the liquid phase [53]. The mixing conditions into the gas particles, identified to droplets after coalescence and dispersion phenomena.

PASR mathematical model:

$$\frac{dy_k^n}{dt} = \frac{1}{m_o \tau R} \sum_{i=1}^{m} \{m_i(Y_{i,k} - \prec Y_k \succ)\} + \frac{Wk\omega k}{\rho^{(n)}} (1)$$

$$\frac{dy^{(n)}}{dt} = \frac{1}{c_p^{(n)} m_o \tau R_i} \sum_{i=1}^{m} m_i \left(\sum_{k=1}^{k_g} Y1,k(h_{i,k} - \prec h_k \succ) \right) - \frac{W_k \omega_k^{(n)} h_k^{(n)}}{\rho^{(n)} c_p^{(n)}} (2)$$

$$-\sum_{\alpha=1,\beta=1}^{K_{tot}} \frac{\partial^2}{\partial \Psi_\alpha \Psi_\beta} \left\{ \left\langle \varepsilon_{\alpha\beta} \mid \overline{\Phi} = \overline{\Psi} \right\rangle \tilde{P}_{\overline{\Phi}}(\overline{\Psi}, t) \right\} = \frac{1}{\tau_{mix}} \left\{ \iint_{\Psi' - \Psi''} \tilde{P}_{\overline{\Phi}}(\overline{\Psi'}, t) \tilde{P}_{\overline{\Phi}}(\overline{\Psi''}, t) H(\Psi', \Psi'' \mid \overline{\Psi}) - \tilde{P}_{\overline{\Phi}}(\overline{\Psi}, t) \right\} (3)$$

$$\sum_{\alpha=1,\beta=1}^{K_{tot}} \frac{\partial^2}{\partial \Psi_\alpha \partial \Psi_\beta} \left\{ \left\langle \varepsilon_{\alpha\beta} \mid \overline{\Phi} = \overline{\Psi} \right\rangle \tilde{P}_{\overline{\Phi}}(\overline{\Psi}) \right\} = \frac{c_\Phi}{\tau_{max}} \frac{\partial}{\partial \Psi_\alpha} \left\{ \left(\overline{\Psi} - \tilde{\overline{\Phi}} \right) \tilde{P}_{\overline{\Phi}}(\overline{\Psi}) \right\} (4)$$

$$\text{unmixedness} = \frac{\overrightarrow{\langle f'' f'' \rangle}}{(1 - \langle \tilde{f} \rangle) \tilde{f} \rangle} \quad (5)$$

$$H(\Psi'\Psi'' = \overline{\Psi}\left\{\frac{1}{|\Psi' - \Psi''} \text{ if } \Psi \notin [\Psi', \Psi''\right]; \quad (6)$$

Otherwise, H: transitional probability

H=0

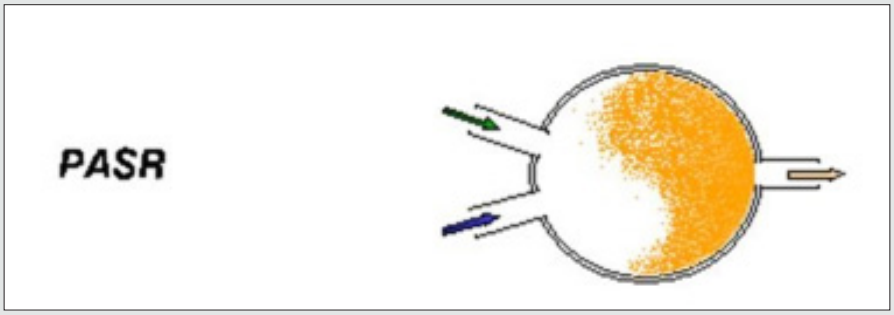

Figure 1: Pilot flame model, a partially stirred reactor.

Table 1: Thermodynamic features of the supplied gaseous fuels.

Fuels Features										
GAS	Chemical Mixture Molar %								PM g/mole	LHV Mj/kg
	CH_4	CO	C_2H_6	C_3H_8	C_4H_{10}	CO_2	H_2	N_2		
Nat Gas	0.92	0	0.037	0.01	0.0025	0.0015	0	0.029	17.34	47.2
Nat Meth	0.95658	0.00089	0.02053	0.00473	0	0	0	0.01727	16.64	51.93
Biogas	0.65	0	0	0	0	0.35	0	0	29.44	32.5
Biom O	0.18	0.33	0.02	0.02	0.02	0.1	0.25	0.08	21.92	19.2
SW gas	0.07	0.61	0.07	0.07	0	0	0.18	0	23.76	21.7

Respectively: (1), (2): mass and energy balance equations; (3): Molecular mixing Curl 's equation; (4) Interaction-by-Exchange-with-the-Mean Linear-Mean Square-Estimation molecular mixing; (5) the un mixedness level, expressed through the density of mixture fraction and the weighted average of the fluctuations, adaptable and differently dependent on the conditions (3), (4). according to the Curl's model H, the transit probability function (6).

Whenever Cϕ = 1/3, the models should produce the same equal un mixedness level, for a given

mixing time range.

$$unmixedness = \frac{1}{1 + \tau_{res} / 3\tau_{mix}} \quad (7)$$

The hypothesis on Damkhöler number: Da = (mixing time)/(reaction time) ≫ 1 indicates a prevalent effect of turbulent mixing time with respect to the reaction time due to the speed of the combustion reactions [54-56]. This of turbulence assures uniformity of the main thermochemical properties.

Evolution of species was investigated via the GRI Mech 3.0 model, that achieves completeness by describing and simulating hydrocarbon combustion and reporting NOx production, resulting in long calculation times recorded by the CPU. A standard dual-core PC, such as that used in this research, takes three days to conduct each simulation run. The complex phenomenon, whose investigation is at a high grade of development and whose descriptive variables were highly uncorrelated, is a Monte Carlo [57-59] problem. Combustion, in fact, involves different species under established operational conditions and very different evolutions (the radical and the molecular reactions). Analytically, this stiff system was solved using the numerical method: backwards difference formula BDF [60-63]. The fundamental choice is on the integration step since the constraint of the stability of the solution was more important than the accuracy. This multi-grid problem [64-68] was approached by evaluating the joint probability [69] of temperature and concentration.

Results

The author [70] investigated about performances of gaseous fuels into 100 KWe MGT according to different paths. The numerical simulation of several biofuels [71] imposing different fluid-dynamic hypothesis, e.g., by comparing those from the partially premixed and the laminar flame let fluid-dynamic models [72]. Focusing on a standard biogas [73,74] from sewage, supplied the 100 kWe MGT, via the k-ε fluid-dynamic model. The latter model, also applied to analyze performances and thermal effects of biomass gas and solid waste gas, in respect to the H_2 content [75,76], in the same 100 kWe MGT. The species H, O, CH_2, CH_2S, and OH were extrapolated as common markers among all the considered kinetic models. The latter were, to remember: the simplest model methane 17, composed of 17 intermediate species of the reaction and 73 chemical reactions; the methane 30, composed of 30 different species and chemical equations; the GRI Mech 3.0, composed of 53 species and chemical equations.

The outcomes recorded in Tables 2-5 below reports about the first simulated steps, proceed via the skeletal kinetic model methane 17 that, due its nature, requires the lower cost on the CPU (Central Process Unit). In the economy of dissertation [77-79], it was decided to report and to select only a part of all the chemical and physical effects and behaviors related to the numerous statistical evaluations that were carried out. e.g.: the hypothesis of the stability of solution, the analysis of what produced a variation of mathematical parameters (DT and n) was neglected in this paper, even though these calculations were performed for completeness [80- 82] of analysis. Several simulations performed: the way was to change each parameter at each run, fixing the others all. The main constraints for defining the optimal operating environment were the partial mixing M_{IXT}, the ignition temperature T, and the fuel: air ratio. These parameters all are interconnected [83-85]. Tables 3-5 below show the outcomes of numerical simulations using various inputs chosen for the parameters of the mathematical model describing the flame characteristics. Operational conditions -pressure, typical temperatures and other features describing the considered PaSR environment of the MGT - on Table 6.

Table 2: Output of simulation under standard conditions.

Heading	H	O	CH_2	CH_2S	OH	Tout	CPU
						[·] = K	h: min:s
$D_T = 5 \times 10^{-5}$	-	-	-	-	-	-	-
n = 2000	-	-	-	-	-		
$f_{stoichiom} = 0.168$	-	-	-	-	-	-	-
$T_{fuel} = 400$ K	3.793×10^{-5}	7.211×10^{-4}	1.779×10^{-7}	1.099×10^{-8}	5.484×10^{-3}	2503	1:29:15
$T_{oxi} = 905$ K							
$T_{init} = 1500$ K	-	-	-	-	-	-	-
$TAU = 15 \times 10^{-3}$	-	-	-	-	-	-	-
$M_{IXT} = 1 \times 10^{-5}$	-	-	-	-	-	-	-

Table 3: Marker's species values, CPU =f (Mathematical parameters).

Mathematical parameters	H	O	CH_2	CH_2S	OH	T_{out}	CPU
						[·] = K	[] = h: min:sec
$D_T = 5 \times 10^{-5}$	-	-	-	-	-	-	-
n = 2000							
$D_{T1} = 2.5 \times 10^{-5}$	n.a.	-	-	-	-	-	-
$D_T = 5 \times 10^{-5}$	3.793×10^{-5}	7.211×10^{-4}	1.779×10^{-7}	1.099×10^{-8}	5.484×10^{-3}	2503	1:29:15
$D_{T2} = 15 \times 10^{-5}$	2.594×10^{-5}	7.366×10^{-4}	-9.619×10^{-14}	-1.181×10^{-14}	5.153×10^{-3}	2443	0:55:05
n = 400	-	n.a.	-	-	-	-	-
n = 1250	7.010×10^{-5}	5.968×10^{-4}	$1.833\ 10^{-15}$	1.466×10^{-16}	5.382×10^{-3}	2564	1:11:19
n = 1500	8.174×10^{-5}	5.164×10^{-4}	$3.387\ 10^{-15}$	2.696×10^{-16}	5.071×10^{-3}	2567	1:10:15
n = 2000	3.793×10^{-5}	7.211×10^{-4}	1.779×10^{-7}	1.099×10^{-8}	5.484×10^{-3}	2503	1:29:15
n = 10000	3.793×10^{-5}	7.211×10^{-4}	1.779×10^{-7}	1.099×10^{-8}	5.484×10^{-3}	2504	1:43:29

Table 4: Marker's species values, CPU =f (Chemical and physical/thermodynamic parameters).

Chemical and physical/thermodynamic parameters	H	O	CH_2	CH_2S	OH	T_{out} [ ] = K	CPU [ ] = h:min:s
$f_{stoichiom}$ = 0.168 T_{oxi} = 905 K T_{init} = 1500 K T [·] = K	-	-	-	-	-	-	-
$f_{stoichiom}$ = 0.168	3.793×10^{-5}	7.211×10^{-4}	1.779×10^{-7}	1.099×10^{-8}	5.484×10^{-3}	2503	1:29:15
f = 1/2f_{stoich} = 0.084	7.189×10^{-7}	1.285×10^{-4}	-1.758×10^{-14}	1.81×10^{-15}	1.194×10^{-3}	2013	0:59:03
f = 0.0625	1.438×10^{-7}	4.839×10^{-5}	1.47×10^{-15}	1.651×10^{-16}	-	1820	0:58:48
f = 0.0572	7.734×10^{-9}	7.357×10^{-6}	3.258×10^{-28}	1.06×10^{-29}	1.379×10^{-4}	1634	0:35:17
T_{fuel} = 300	3.637×10^{-5}	6.961×10^{-4}	1.708×10^{-7}	1.05×10^{-8}	5.366×10^{-3}	2496	2:14:16
T_{fuel} = 400	3.793×10^{-5}	7.211×10^{44}	1.779×10^{-7}	1.099×10^{-8}	5.484×10^{-3}	2503	1:29:15
T_{fuel} = 600	4.167×10^{-5}	7.803×10^{-4}	1.968×10^{-7}	1.217×10^{-8}	5.757×10^{-3}	2520	1:26:32
T_{fuel} = 800	4.634×10^{-5}	8.531×10^{-4}	2.242×10^{-7}	1.391×10^{-8}	6.082×10^{-3}	2539	1:51:37
T_{oxi} = 650	1.944×10^{-5}	4.118×10^{-4}	1.667×10^{-7}	1.023×10^{-8}	3.854×10^{-3}	2386	1:01:19
T_{oxi} = 800	2.890×10^{-5}	5.734×10^{-4}	1.729×10^{-7}	1.391×10^{-8}	6.082×10^{-3}	2456	1:48:02
T_{oxi} = 905 K	3.793×10^{-5}	7.211×10^{-4}	1.779×10^{-7}	1.099×10^{-8}	5.484×10^{-3}	2503	1:29:15
T_{init} = 1000 K	2.273×10^{15}	6.455×10^{15}	1.889×10^{-25}	2.52×10^{-26}	3.313×10^{-15}	823	0:33:02
T_{init} = 1500 K	3.793×10^{-5}	7.211×10^{-4}	1.779×10^{-7}	1.099×10^{-8}	5.484×10^{-3}	2503	1:29:15
T_{init} = 2000	3.970×10^{-5}	7.495×10^{-4}	1.792×10^{-7}	1.108×10^{-8}	5.616×10^{-3}	2511	1:24:31

Table 5: Marker's species values, CPU =f (Fluid-mechanical parameters (of control)).

Fluid-mechanical parameters	H	O	CH_2	CH_2S	OH	T_{out} [·] = K	CPU [] = h: min:sec
$TAUM_{IXT}$	-	-	-	-	-	-	-
TAU = 1×10^{-2}	-	-	-	-	-	-	1:04:13
TAU = 1.5×10^{-2}	3.793×10^{-5}	7.211×10^{-4}	1.779×10^{-7}	1.099×10^{-8}	5.484×10^{-3}	2503	1:29:15
TAU = 2×10^{-2}	2.300×10^{-5}	6.719×10^{-4}	1.596×10^{-7}	9.732×10^{-9}	4.959×10^{-3}	2458	1:25:42
M_{IXT} = 1×10^{-9}	-	-	-	-	-	1500	n.a.
$M_{IXT\ PSR}$ = 1×10^{-7}	5.247×10^{-5}	6.985×10^{-4}	5.195×10^{-16}	4.066×10^{-17}	5.661×10^{-3}	2548	2:23:13
$M_{IXT\ standard}$ = 1×10^{-5}	3.793×10^{-5}	7.2112×10^{-4}	1.779×10^{-7}	1.099×10^{-8}	5.484×10^{-3}	2503	1:29:15
M_{IXT} = 8×10^{-4}	2.683×10^{-5}	2.825×10^{-4}	8.490×10^{-7}	4.772×10^{-8}	2.414×10^{-3}	2130	-
$M_{IXT\ PaSR}$ = 5×10^{-4}	1.181×10^{-5}	2.665×10^{-4}	4.226×10^{-7}	2.379×10^{-8}	2.246×10^{-3}	2124	0:45:11
M_{IXT} = 1×10^{-4}	2.546×10^{-5}	6.362×10^{-4}	1.203×10^{-7}	7.347×10^{-9}	4.791×10^{-3}	2437	1:08:16
$M_{IXT\ PFR}$ = 1×10^{-3}	1.929×10^{-5}	2.308×10^{-4}	5.517×10^{-7}	3.081×10^{-8}	1.989×10^{-3}	2033	0:22:43

Table 6: Parameters at optimal conditions.

MGT Combustion Chamber Partially Premixed Model		
D_T Integration Step	-	5×10^{-5}
n Particle Number	-	2000
M_{IXT} Mixing Time	-	5×10^{-4}
TAU Residence Time	[·] = s	15×10^{-3}
T_{init} Mixing temperature	[·] = K	1200/1300
T_{air} Inlet air temperature	[·] = K	905
T_{fuel} Inlet fuel temperature	[·] = K	400
Other thermodynamic features		
Pressure	3.8 bar	
Q	800 g/s	
Molar Concentrations of involved specie		
standard conditions	$CH_4/H_2 = 0.5$	

The PaSR model uses interactions by exchanging them with the mean as a turbulent moment closure to simulate finite time micro-mixing. Ideal macro-mixing was assumed as characterized by an exponential residence time distribution. The local conditions were relaxed toward the mean at a rate defined by the mixing frequency that was a ratio of turbulent dissipation to turbulent mixing energy. These considerations explain the reason why M_{IXT} is one of the fundamental parameters for finding the optimal operational environment. The numerical values and the shapes of oscillations of the variances [86,87], of the MIXT fluid-dynamic parameter identified the partial mixing. Full mixing [88], reproduced by the Perfect Stirred Reactor (PSR) model is given from very dense, oscillating gaits of the variance of MIXT, as seen in Figure 2 below. If the oscillations of the variance of M_{IXT} are regular (not too deep and not too narrow and short) they suggest partial mixing PaSR model, see Figure 3. Instead, the flat profile observed in Figure 4 is related to the higher numerical values of the variance of MIXT; it was reproduced in the absence of mixing by a Plug-Flow Reactor (PFR). Numerical conclusions, coupled with technical and literary knowledge [89], let us deduce the following optimal numerical values to define the ignition condition of a pilot flame:

a) The partial mixing condition value: $M_{IXT} = 5 \times 10^{-4}$.

b) The ignition temperature [86], T_{init} = 1200/1300 K, depending on the fuel.

c) The ratio of lean fed: $\varphi i = mfuel = 1/2\ \varphi stoichiometric$.

The Thermal profiles were identical when the chemical evolutions related to the processes, they reproduce were similar see Figure 5. By dividing the time of the investigation into three ranges (0-0.05) s, we get the following:

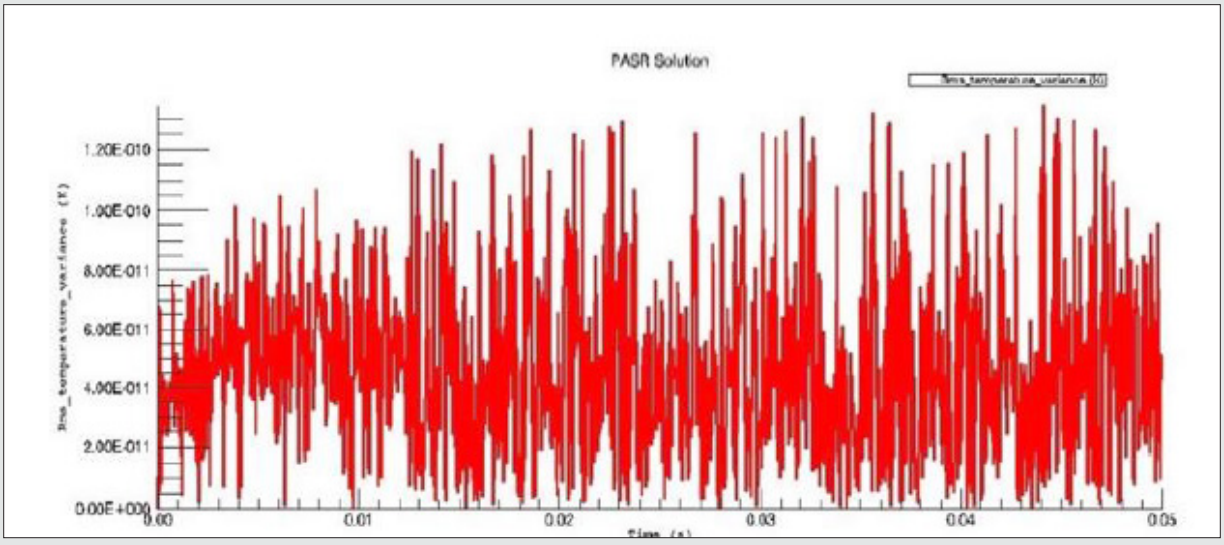

Figure 2: M_{IXT} 1× 10^{-7}-Perfectly Stirred Reactor (PSR) behavior from simulation.

a) (0-0.004) s.

b) (0.004-0.02) s.

c) (0.004-0.05) s.

Graphical representations of the temperature evolutions of methane 17 and GRI Mech 3.0 perfectly overlap within the first and the last range of time, whereas they show a hysteresis within (0.004-0.02) s. GRI Mech 3.0 evolution proceeded at a lower temperature in the indicated last range of time. This likely depends on the absorption of energy because of the endothermic reactions of the NO_x compounds have been calculated. They produce a bulk lowering of temperatures. Thermal profiles of Methane 17 and Methane 30 totally overlap under the considered conditions [Figure 6].

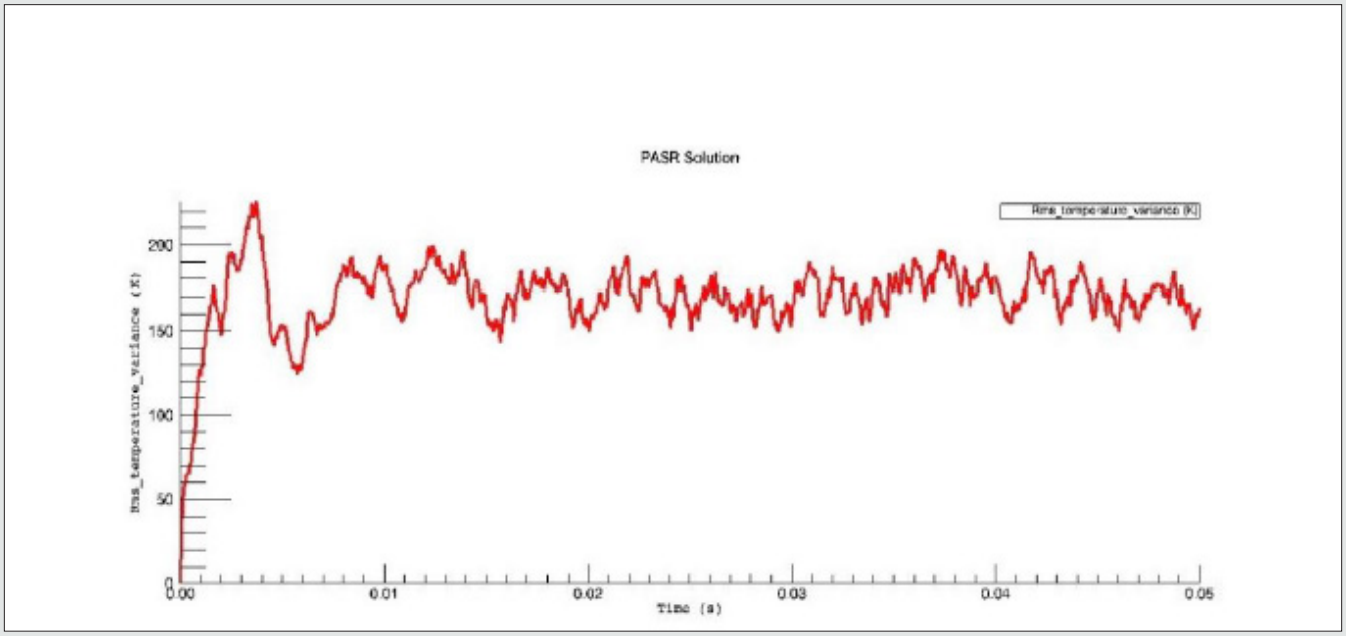

Figure 3: M_{IXT} 1×10^{-4}-Partially Stirred Reactor (PaSR) behavior from simulation.

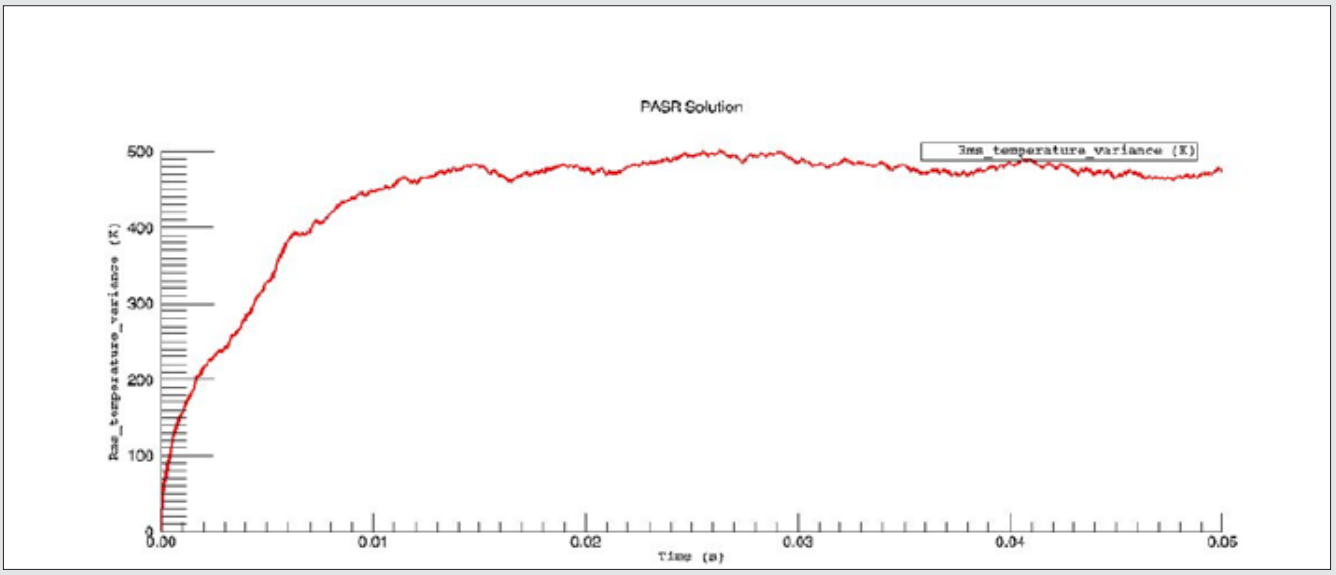

Figure 4: M_{IXT} 1×10^{-3}-PFR (Plug-Flow Reactor) behavior from simulation.

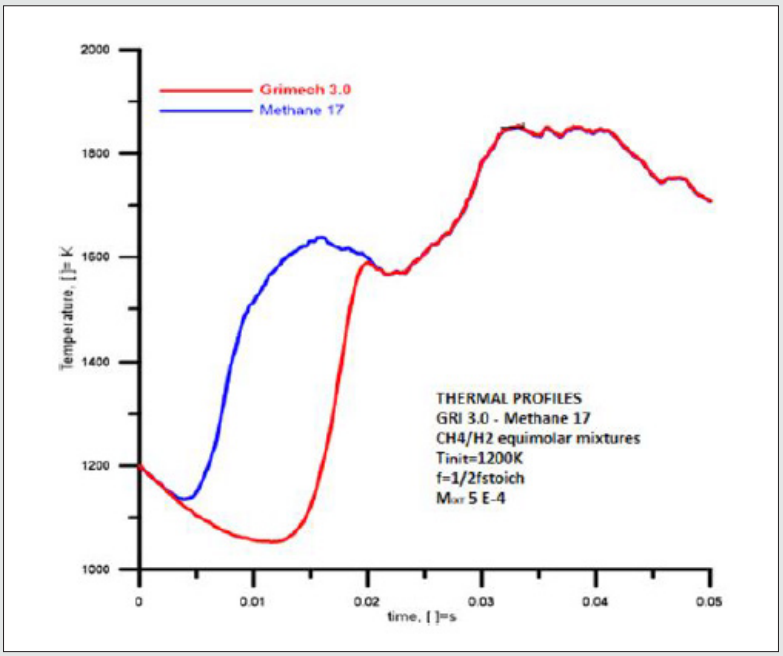

Figure 5: Methane 17; GRI Mech 3.0 optimal condition.

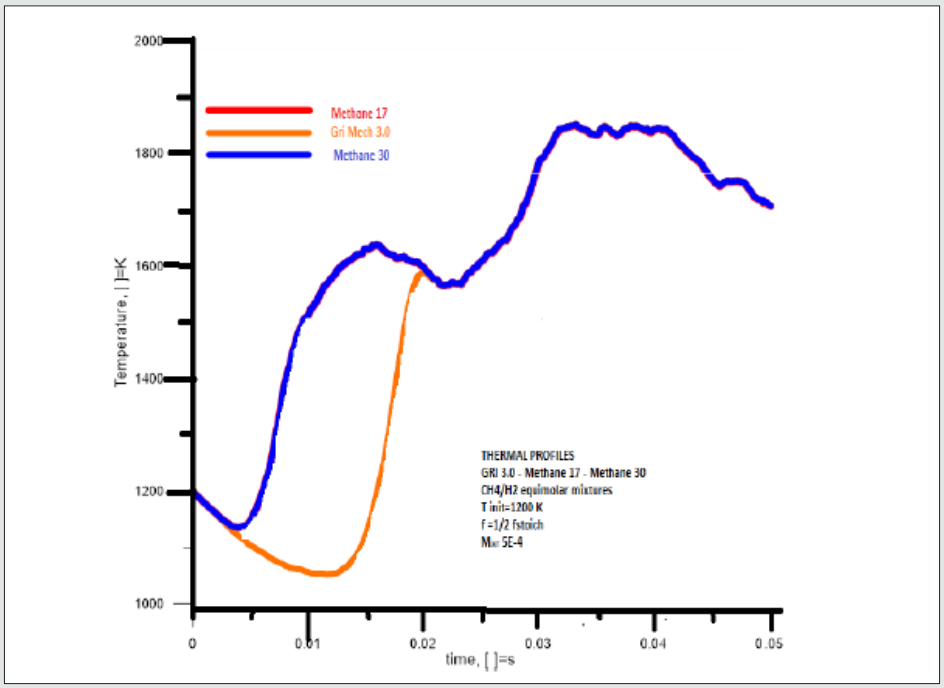

Figure 6: Methane 17; Methane 30; GRI Mech 3.0 optimal condition.

Results and Discussion: NOx Production

In the path of previous investigations about NO_x production [90, 91], and focusing on from micro gas-turbines, [92-94], it was developed the idea of a privileged and simplified way to calculate it [95], by evaluating the "relative abundances" of the intermediates of the production of NO_x [96,97], compounds. The most well-known kinetic outputs related to the reaction mechanisms of NO_x [98, 99], were via the flame or post-flame steps. Conversions according to the flame Zeldovich mechanism, increases the NO yield, also reinforced via the prompt mechanism; the weaker contribution on NO yield comes from NNH, reaction mechanism. In comparison, the H atomic [100], attack reaction on that of the N_2O balance, the O atomic balance attack on N_2O balance, and the Zeldovich

mechanism via the O atomic balance attack reaction on molecular N_2 are of the post-flame production. The kinetic mechanisms of NO_x production are described in Table 7: In the second part of the study, it was considered that the gaseous fuels were supplied at the optimal conditions previously found - the fluid-dynamic parameter M_{IXT}; the fuel/air ratio and the ignition temperature T. By imposing kinetic constraints on the NO_x production [101], the focus is to extrapolate an autonomous, simple reduced kinetic mechanism or, better, a schema, of its evaluation and computing. By using the GRI Mech 3.0 model, were simulated, by running, behaviors of natural gases, but also of biomass gas: solid waste gas and biogas, of which the compositions on Table 1.

Table 7: The kinetic mechanisms of NOx production.

Zeldovich mechanism	**Nitrous oxide mechanism**
1. rxn 1 N2 + O ⟹ NO + N	1. rnx 4 N2 + O + M ⟹ N2O + M
2. rxn 2 N + O2 ⟹ NO + O	2. rnx 5 N2O + O ⟹ NO + NO
3. rxn 3 N + OH ⟹ NO + O	3. rnx 6 N2O + H ⟹ NO + NH
*Kinetics relation: $\frac{d[NO]}{dt}=2k_1[N_2][O]$	*Kinetic equation: $\frac{d[NO]}{dt}=2k_7[N_2][CH]$ supposing quantitative oxidation of HCN and N to NO and N that react according to rxn 2 and rxn 3 reactions.
NO prompt mechanism	**NNH mechanism**
1. rnx 7 N2 + CH ⟹ HCN + N	1. rnx 8 N2 + H ⟹ NNH + H 2. rnx 9 N2 + H + M ⟹ NNH + M 3. rnx 10 NNH + O ⟹ NO + NH 4. rnx 11 NNH + O ⟹ N2O + OH
kinetic relation: $\frac{d[NO]}{dt}=2k2k_5[N_2O][O]+2k_6[N_2O][H]$ *Quantitative oxidation of NO to NH was supposed. Not reported, because of conciseness questions, N_2O and N_2 reconversion reactions.	*Kinetic relation: $\frac{d[NO]}{dt}=2k_{10}[NNH][O]$ are the same defined by Miller and Bowman at the end of 1880, except for the NNH mechanism, pointed out by Bozzelli and Dean in 1995.

Table 8: Concentrations of the main intermediate and/or product of NOx production.

Kinetic Analysis-NO_x Precursors Concentrations, by Varying Fuels and the Operating Optimized Temperature						
CH	**N_2O**	**NNH**	**O**	**H**	**NO**	**Gas at the ignition temperature**
2.406×10^{-9}	1.041×10^{-6}	2.094×10^{-9}	2.232×10^{-4}	9.245×10^{-6}	1.557×10^{-3}	Natural gas T = 1300 K
-1.545×10^{-27}	3.245×10^{-11}	3.298×10^{-18}	6.259×10^{-13}	1.256×10^{-13}	1.055×10^{-17}	Natural gas T = 1200 K
2.966×10^{-10}	6.436×10^{-7}	3.516×10^{-10}	3.383×10^{-5}	1.733×10^{-6}	2.031×10^{-4}	Biomass O gas T = 1200 K
1.594×10^{-10}	8.027×10^{-7}	5.569×10^{-10}	7.565×10^{-10}	2.576×10^{-6}	6.251×10^{-4}	SW gas T = 1200 K
6.016×10^{-12}	1.659×10^{-6}	1.080×10^{-11}	1.165×10^{-5}	7.072×10^{-6}	3.035×10^{-6}	Biogas T = 1300 K
-4.569×10^{-30}	5.299×10^{-12}	1.542×10^{-19}	2.856×10^{-13}	5.743×10^{-6}	9.034×10^{-18}	Biogas T = 1200 K

Table 9: CO_x-NO_x emissions produced under the optimal conditions of a pilot flame (PaSR) of a 100 kWe MGT.

Emissions: CO-CO_2, NO-NO_2, Ignition T, and Final T at a Pilot Flame					
CO	**CO_2**	**NO**	**NO_2**	**Tout [·] = K**	**Gas at the ignition temperature**
6.802×10^{-3}	9.238×10^{-2}	1.557×10^{-3}	7.992×10^{-6}	2100	Natural Gas NG T 1300 K
1.688×10^{-2}	1.147×10^{-1}	2.256×10^{-3}	1.613×10^{-6}	2244	Natural Gas NG T 1200 K
4.815×10^{-3}	7.966×10^{-2}	2.031×10^{-4}	2.810×10^{-6}	1622	Biomass gas (O) T 1200 K
7.358×10^{-3}	1.074×10^{-1}	6.251×10^{-4}	4.807×10^{-6}	1826	SW gas T 1200 K
3.982×10^{-4}	6.483×10^{-2}	3.035×10^{-6}	2.303×10^{-7}	1435	Biogas T 1300 K
9.137×10^{-8}	2.727×10^{-2}	8.631×10^{-18}	3.456×10^{-17}	876	Biogas T 1200 K

As in the identification of the optimal conditions of the pilot flame at ignition, some intermediate agents were markers to evaluate chemical kinetic developments. The selected species [102], thought to be the most significant and essential, are CH, NO_2, NNH, OH, H, and NO. They motivation of this choice is because they interconnect the three considered kinetic mechanisms of gaseous hydrocarbon combustion. More information about the thermodynamic conditions at ignition, related to the different fuels, is shown in Table 8. By computational simulation, it can be concluded that natural gas and biogas, mainly made from a carbon matrix, ignite at T_{init} = 1300 K, whereas the ignition temperature of solid waste and biomass gas is T_{init} = 1200 K. The lower ignition temperature of the latter gases is because of the H_2 percentage in the mixture. When it burns, gases made of a part of H_2, releases the higher energy amount of H_2 contribute into the reaction bulk.

An expected evolution of combustion is that it proceeds with a constantly burning flame, whereas an unsolicited evolution of a good combustion is the flame extinction. The condition of flame extinction is given by the absence of a correlation between the statistical variable's temperature and concentration. The negative value of the dependent variable CH underlines and expresses the almost absence of statistical correlation (see Table 8, which reports statistical evolutions of the main species involved in the NOx production in a gaseous combustion, according to schemas proposed on Table 7 between CH production at the ignition temperature T=1200K for biogas or for natural gases. The CH species, in a chemical-physical point of view, it is as if that which supports the ignition and the advancement of combustion. The minimum production of NOx species is because of the globally warm environment, and not due to a real burning. Table 9 shows show the final outcomes in terms of CO_x and NO_x and temperatures achieved by the different gases, at the established ignitions temperatures. The Table 9 reports the global CO, CO_2, NO, NO_2 productions and the final temperatures, considering the different supplied gas at their own related ignition temperatures Natural gas has the highest LHV; its combustion produces the highest amount of NO_x compounds, including NO, since this production is endothermic. The second most abundant compound produced was N_2O [103], Natural gas, biogas, and methane-based production produced N_2 Almost 1×10^{-7} at an ignition temperature T_{init} = 1300 K. Biomass gas [104], solid waste gas, and H_2-based production produced a similar amount of N_2O at a lower ignition temperature T_{init} = 1200 K.

At T_{init} = 1200 K:

a) $[N_2O_2]$ natural gas = 1×10^{-11}.

b) $[N_2O]$ biogas = 1×10^{-12}.

The lower ignition temperature depended on the high amounts of energy released by the H_2 of the mixture during its combustion.

The NNH compound was produced mainly by the flame from each fuel at its own ignition temperature:

a) [NNH]NG ≈ 1×10^{-9}.

b) [NNH]biomass gas-solid waste gas ≈ 1×10^{-10}.

c) [NNH]biogas ≈ 1×10^{-11}.

The intermediate species CH monitors HCN production and was developed via the prompt, mechanism. The lowest concentration of it was produced by burning biogas: [CH] biogas ≈ 1×10^{-12}. This kinetic outcome confirms the previous evaluations [73], about the developments of the fluid dynamic of biogas combustion, according to the k-ε model into the burner of a 100 kWe MGT. It was discovered, in that case, and here it was not applied, a higher flow, three times the standard, to perform biogas combustion.

Biogas reached a final temperature T_{out} = 1435 K. The global thermal balance, $\Delta T = T_{out} - T_{mix} = 145$, shows a very small amount of energy, useful only for warming up the reactive bulk into the burner. The overheated environment just promoted a slight NO_x production, mainly by means of the flame mechanism.

Results and Discussion: Hydrocarbons, NO_x, and Kinetic Mechanisms

Many scientists investigate on the GRI Mech mechanism, to discover and extrapolate consistent and streamlined congruent paths. If the GRI Mech model, written in Fortran, is the most complete to evaluate kinetic schema of gaseous fuel combustion, it also requires long calculation times to run the reported survey points to validate a more synthetic schema by extrapolating the common representative intermediates among those of the showed kinetic models: from the simplest, to the GRI Mech 3.0. The latter, which includes species heavier than methane, other low molecular weight hydrocarbons, it is the only one in which are all the species of NO_x production. It is the most complete but, as understandable since the hypothesis, also the heaviest in computation The subroutine below shows the extrapolated simplified schema of a generic gaseous hydrocarbon input. This schema, obtained by subtracting the minimum number of significant and common H/C compounds from the three models: methane 17, methane 30, and GRI Mech 3.0, is to provide an independent and simple evolution model of nitrogen oxides: a new input of calculation.

Input of NOx production

ELEMENTS

O H C N AR

END

SPECIES

H_2 H O O_2 OH H_2O HO_2 H_2O_2 C CH

CH_2, CH_2S, CH_3, CH_4, CO, CO_2, HCO, CH_2O, CH_2OH, HCCOH N, NH

NH_2 NH_2 NNH NO NO_2 N_2O HNO CN

HCN H_2CN HCNN HCNO HOCN HNCO NCO N_2

AR C_3H_7 C_3H_8 CH_3CHO

END

Conclusions and Further Developments

The numerical investigation on thermo fluid dynamics about the ignition of the pilot flame of a 100 kWe MGT has find out some optimal operational conditions to reproduce the Partially Stirred Reactor. Optimal operational conditions were investigated, related to the practical application of different fuels, and focused by the fluid-dynamic parameter M_{IXT}; the temperature at the start of combustion, T_{init}; and the best ratio for feeding that well reproduces the environment of analysis into values:

a) $^{M}IXT = 5 \times 10^{-4}$

b) T_{init} = 1200/1300 K, depending on fuel

c) lean fed: φi = *mF*uel= 1/2 φstoichiometric.

These values were identified by a very analytical cross-study - a certain sense almost a sort of hand-made investigation- among the kinetic model's methane 17, methane 30, and GRI Mech 3.0. The graphical overlap of the thermal profiles among those models, then the hysteresis, show their kinetic connections. The "GRI Mech 3.0" kinetic model, at hysteresis, proceeded at lower values of temperature with respect to those of methane 17 and methane 30. It is very likely that this shows, depending on its completeness, the NO_x endothermic production effect. M_{IXT} is the control fluid-dynamic parameter, and the constraining of partial mixing, as evidenced by means of the oscillations of the variation in temperature, which are fully dumping the perfect stirred; asymptotic, the partial mixing; or flat as the plug flow path. The ignition temperature $T_{init} = T_{mix}$ and the feed ratio depend on the composition of the mixtures of the supplied fuels. At a fixed feed ratio, the T_{init} was lower when the fuels had a higher LVH or if the species of which they were made of were very energetic and burnt fast. The H_2 composition of the biomass gas and solid waste gas let them ignite at a lower temperature (T_{init} = 1200 K). A kind of skeletal model for the synthesis of NO_x compounds from the three kinetic models considered was obtained by abstraction and by considering their connection species in a sort of analysis of the main PCA components.

H O OH H_2O HO_2 H_2O_2 C
CH

CH_2 CH_2S CH_3 HCO CH_2O CH2OH HCCOH
N NH

NH_2 NH_3 NNH NO NO_2 N_2O HNO
CN

HCN H_2CN HCNN HCNO HOCN HNCO NCO

AR

A remarkable further outcome about the Biogas that produced the lowest NO_x concentration among all the investigated gaseous fuels. This information reinforced a previous conclusion about biogas; it needs a higher flow rate to burn. At the ignition T_{init}, in fact, its global thermal energy balance, $\Delta T = T_{out} - T_{mix}$ = 145, was very low and was insufficient to support combustion, although it was enough to warm the flow and produce endothermic NO_x. The future goal is to improve those conclusions, input data, and quantifying the benefit of the CPU. At embryo stage, the identification of the most fitting and simple kinetic model in terms of C/H ratio, to connect to the simplified NOx production model. Considering the power generation from H_2 in near future, all conclusions obtained at now will be reproduced to achieve performances evaluations at the two feedings of pure H_2 and in ever richer NG- H_2 blends.

Highlights

a) Biofuels and partially Stirred Reaction conditions of combustion.

b) Connecting points and overlapping of outcomes among the kinetic model's methane 17.

c) methane 30; Gri Mech 3.0

d) Significant operational conditions describing environment of partially stirring.

e) Idea of a smarter simplified model to calculate NO_x.

Funding

This research received no external funding.

Conflicts of Interest

The authors declare no conflicts of interest.

References

1. Minghetti E (2016) La turbine a gas: tecnologie attuali e sviluppi future. RT/ERG/96/29; ENEA, Centro Ricerche Casaccia: Rome, Italy 28(23).
2. Bartolo G (2009/2010) Cogenerazione su piccola scala, Degree Thesis, Chapt. 3 Le Microturbine a Gas, a.y. 2009/2010http://hdl.handle.net/10589/6341
3. Law CK (2006) Combustion Physics. Cambridge University Press: Cambridge
4. Smith GP, Golden DM, Frenklach M, Moriarty NW, Eiteneerc B, et al. The GRI-MechTM Model for Natural Gas Combustion and NO Formation and Removal Chemistry,
5. Borghi R (1990) Gas turbine combustion" Lecture Notes; Von Karman Institute for Fluid Dynamics: Sint-Genesius- Rode, Belgium.
6. Flamme M (2004) New Combustion Systems for Gas Turbines (NGT). Applied Thermal Engineering, 24(11-12): 1551-1559.
7. Cameretti MC, Tuccillo R (2005) Combustion, and combustor for MGT application, Microgas turbines educational notes, NATO/PFP UNCLASSIFIED; RTO-EN-AVT-131 5: 1-56.
8. Peters N (2000) Turbulent Combustion, Monographs on Mechanics, Turbulent Combustion. Cambridge University Press: Cambridge
9. Turns SR (2012) An Introduction to Combustion, Concept and Application, 3rd (eds) Mc Grow Hill Educations: Nuova Dheli, India
10. Andreini A (2004) Sviluppo di modelli numerici per l'analisi della combustione turbolenta premiscelata in microturbine a gas. Ph.D. Thesis, Energetica e Tecnologie Industriali Innovative, University of Florence
11. Canova A, Chicco G, Genon G, Mancarella P (2008) Emission characterization and evaluation of natural gas-fueled cogeneration microturbines and internal combustion engines. Energy Conversion and Management 49(10): 2900-2909.

12. Persico G, Pini M (2017) Fluid dynamic design of Organic Rankine Cycle Turbines. Organic Rankine Cycle (ORC) Power Systems: Technologies and Applications, Woodhead Publishing pp. 253-297.
13. Gobbato P (2010) Studio Delle Instabilità Termoacustiche in un Combustore di Microturbina a Gas. (Ph. D Thesis) Industrial Engineering, Energy Engineer, University of Padova
14. Li Y, Wang P, Wang S, Liu J, Xie Y, et al. (2019) Quantitative investigation of the effects of CR, EGR and spark timing strategies on performance, combustion and NOx emissions characteristics of a heavy-duty natural gas engine fueled with 99% methane content. Fuel 255: 115803.
15. Sankaran R, Hawkes ER, Chen JH, Lu TF, Law CK, et al. (2007) Structure of a spatially developing turbulent lean methane-air Bunsen flame. Proceedings of the Combustion Institute 31(1): 1291-1298.
16. Lu T, Law CK (2008) A Criterion Based on Computational Singular Perturbation for the Identification of Quasi Steady State Species: A Reduced Mechanism for Methane Oxidation with NO Chemistry. Combustion and Flame 154(4): 761-774.
17. Schwer DA, Lu P, Green WH Jr (2003) An adaptive chemistry approach to modeling complex kinetics in reacting flows. Combustion and Flame 133(4): 451-465.
18. Lam SH, Goussis DA (1988) Understanding complex chemical kinetics with computational singular perturbation22nd Symposium (International) on Combustion. Pittsburg: The Combustion Institute pp. 931-941.
19. Lam SH (1993) Using CSP to Understand Complex Chemical Kinetics. Combustion Science Technology 89(5-6): 375-404.
20. Nicolini P (2007/2008) Separazione delle scale temporali e "Slow Manifolds": elementi per la riduzione di dimensionalità nella descrizione delle cinetiche chimiche. Tesi di laurea specialistica in chimica, Università degli Studi di Padova.
21. De Luca G (2001) Montecarlo Methods, Reading Seminar Metodo montecarlo,Università degli Studi di Roma Tor Vergata.
22. Baffa Scirocco T, Fiorino E, Pelacchi P, Poli D (2006) A Monte Carlo technique for setting operating reserve margins under network constraints. ,9^ International Conference on Probabilistic Methods Applied to Power Systems 1: 6.
23. Briggs WL, Henson VE, McCormick SF (2000) A Multigrid tutorial, Tutorial -2 edition. SIAM
24. Diskin B, Thomas JL, Mineck RE (2005) On quantitative analysis methods for multigrid Solutions, SIAM J Sci Computing 27(1): 108-129.
25. Di Franco G (2017) Tecniche e modelli di analisi multivariate, La cassetta degli attrezzi per le scienze umane, 8, (Eds). Franco Angeli pp. 304.
26. Frassoldati A, Faravelli T, Ranzi E (2003) Kinetic modeling of the interactions between NO and hydrocarbons at high temperature, Combustion and Flame 135(1-2): 97-112.
27. Cuoci A, Frassoldati A, Ferraris GB, Faravelli T, Ranzi E, et al. (2007) The ignition, combustion, and flame structure of carbon monoxide/ hydrogen mixtures. Note 2: Fluid dynamics and kinetic aspects of syngas combustion. International Journal of Hydrogen Energy 32 (15): 3486-3500.
28. Kasuya F, Glarborg P, Johnsson JE, Dam-Johansen K (1995) The thermal De-NOx process: Influence of partial pressures and temperature, Chemical Engineering Science 50 (9): 1455-1466.
29. Valorani M, Creta F, Goussis DA, Lee JC, Najm HN, et al. (2006) An automatic procedure for the simplification of chemical kinetic mechanisms based on CSP. Combustion and Flame 146(1-2): 29-51.
30. Fraser SJ (1998) The steady state and equilibrium approximations: A geometrical picture,The Journal of Chemical Physics 88(8): 4732-4741.
31. Rousseland MR, Fraser SJ (1990) Geometry of the steady-state approximation: Perturbation and accelerated convergence methods. The Journal of Chemical Physics 93(2): 1072-1081.
32. Keck JC (1990) Rate-controlled constrained-equilibrium theory of chemical reactions in complex systems. Progress in Energy and Combustion Science 16(2): 125-154.
33. Maas U, Pope SB (1992) Implementation of simplified chemical kinetics based on intrinsic low-dimensional manifolds. Simpoium (International) on Combustion 24(1): 103-112.
34. Gol'dshtein VM, Sobolev VA (1992) Singularity Theory and problems of functional analysis, Qualitative analysis of Singular Perturbated Systems of Chemical Kinetics, American Mathematical Society Translations 153: 73-92.
35. Lu T, Law CK (2008) A Criterion Based on Computational Singular Perturbation for the Identification of Quasi 518 Steady State Species: A Reduced Mechanism for Methane Oxidation with NO Chemistry. Combustion and Flame 154(4): 761-774.
36. Lu T, Law CK (2008) Strategies for mechanism reduction for large hydrocarbons: n-heptane, Combustion and Flame 154(1-2): 153-163.
37. Bendtsen AB, Glarborg P, Dam-Johansen K (2001) Visualization Methods in Analysis of Detailed Chemical Kinetics Modeling. Computers & Chemistry 25(2): 161-170.
38. Tham YF, Chen JY (2003) Recent Advancement on Automatic Generation of Simplified Mechanism, Western States Section/Combustion Institute. WSS-CI, paper 03F-49.
39. Liu F, Guo H, Smallwood GJ (2002) The chemical effect of CO2 replacement of N2 in air on the burning velocity of CH4 and H2 premixed flames, Combustion and Flame 133: 495-497.
40. Klippenstein SJ, Harding LB, Glarborg P, Miller JA (2011) The role of NNH in NO formation and control. Combustion and Flame 158(4): 774-789.
41. Bhattacharjee B, Schwer DA, Barton PI, Green WH Jr (2003) Optimally reduced kinetic models: reaction elimination in large-scale kinetic mechanisms. Combustion and Flame 135(3): 191-208.
42. Vajda S, Valko P, Turanyi T (1985) Principal component analysis of kinetic models. International Journal of Chemical Kinetics 17(1): 55-81.
43. Beek J, Miller RS (1959) Turbulent transport in chemical reactors. Chemical Engineering Progress Symposium 55(25): 23-28.
44. McKelvey KN, Yieh HN, Zakanycz S, Brodkey RS (1975) Turbulent motion, mixing, and kinetics in a chemical reactor configuration. AIChE Journal 21(6): 1165-1176.
45. Levenspiel O (1962) Mixed models to represent flow of fluids through vessels. The Canadian Journal of Chemical Engineering 40(4): 135-138.
46. Himmelblau DM, Bischoff KB (1963) New development in mass transfer. Industrial & Engineering Chemistry 55(10): 50-57.
47. Mahendra Reddy V, Biswas P, Garga P, Kumar S (2014) Combustion characteristics of biodiesel fuel in high recirculation conditions. Fuel Process Technology 118: 310-317.
48. Chang LJ, Metha RV, Tarbell JM (1986) An Evaluation of Model of Mixing and Chemical Reaction with a Turbulence Analogy. Chemical Engineering Communication 42(1-3): 139-155.
49. Curl RL (1963) Dispersed phase mixing: I. Theory and effects in simple reactors. AIChE Journal 9(2): 175-181.
50. Miller RS, Ralph JL, Curl RL, Towell GT (1963) Dispersed phase mixing: II. Measurements in organic dispersed systems. AIChE Journal 9(2): 196-202.
51. Chatzi E, Lee JM (1987) Analysis of interactions for liquid-liquid dispersions in agitated vessels. Industrial & engineering chemistry research 26(11): 2263-2267.

52. Salvadori MG, Baron ML (1962) Numerical Methods in Engineering, 2nd (eds) Prentice-Hall,Eglewoods Cliffs NJ 75-79.

53. Tangirala V, Haynes J, Correa S.M, Seiser R (2002) Numerical Simulation of Late-Lean Ignition Processes, Technical Report 2001CRD210; GE Research and Development Center: New York, NY, USA.

54. Bourne JR, Kozicki F, Rys P (1981) Mixing and fast chemical reaction-I: Test reactions to determine segregation. Chemical Engineering Science 36(10): 1643-1648.

55. Cetnar J, Gudowski W, Wallenius J MCB: a continuous energy Monte Carlo burnup simulation code. in actinide and fission product partitioning and transmutation 523-527.

56. AAVV⟦MCNP⟧^TM- A general Montecarlo N-particle transport code. Version 4C; Judith F., Briesmeister Eds.

57. Treleaven CR, Tobgy AH (1972) Monte Carlo methods of simulating micromixing in chemical reactors. Chemical Engineering Science 27(8): 1497-1513.

58. Petrovich C (2001) SP-FISPACT, A computer code for activation and decay calculations for intermediate energies. A connection of FISPACT with MCNPX.

59. Brenan KE, Engquist BE (1988) Backward differentiation approximations of nonlinear Differential/Algebraic Systems. Mathematics of Computation 51(184): 659-676.

60. Fredebeul C (1998) A-BDF: A generalization of the Backward Differentiation Formulae. SIAM, Journal on Numerical Analysis 35(5): 1917-1938.

61. Lötstedt P, Petzold L (1986) Numerical solution of nonlinear differential equations with algebraic constraints. I. Convergence results for backward differentiation formulas, Mathematics of Computation 46(174): 491-516.

62. Brandt A, McCormick SF, Ruge JW (1983) Multigrid Methods for Differential Eigenproblems, SIAM, Journal of Scientific and Statistical Computing 4(2): 244-260.

63. Ruge J, Stuben K, McCormick SF (1987) Algebraic Multigrid, Multigrid Methods SIAM pp. 73-130.

64. South JCJr, Brandt A, Application of a multi-level grid method to transonic flow calculations, Technical Report. Numerical Analysis, NASA-TM-81066, ICASE-76-78.

65. Stuben K (1963) Algebraic multigrid (AMG): experiences and comparisons, Applied Mathematics and Computation 13(3-4): 419-451.

66. Brandt A, Livne OE (2011) Multigrid Tecnique: 1984 Guide with Application to Fluid-dynamic. Revised Edition SIAM, Applied Mathematics, 21: 201.

67. Molteni L, Manoforte R (2014) La conjoint analisis Liuc Papers in 58, Serie Metodi Quantitativi 8,1998.

68. Liguori V Studio delle fenomenologie di combustion di miscele gassose in microturbine a gas, Ph.D. Thesys, Engineering of Mechanical Systems, 2014, XXVI Course, Department of Industrial Engineering, University of Naples "Federico II".

69. Iturbe Hernández, Guzmán JEV, Vicente W, Salinas Vazquez M (2020) Microturbine characteristics and emissions using biofuel blends. Biofuels.

70. Liguori V (2014) Laminar flamelet partially premixed combustion model in a MGT: new fuels performances and emissions, Energy Procedia 45: 1432-1441.

71. Liguori V (2016) Numerical investigation: Performances of a standard biogas in a 100 kWe MGT. Energy Report 2: 99-106.

72. Bazooyar B, Darabkhani HG (2019) Design Procedure and Performance Analysis of a Microturbine Combustor Working on Biogas for Power Generation. ASME Turbo Expo 2019: Turbomachinery Technical Conference and Exposition, Volume 4B: Combustion, Fuels, and Emissions.

73. Liguori V (2017) Biomass gas and solid waste gas lean premixed combustion in a 100 kWe MGT: A numerical investigation considering their H2 percentage, International Journal of Hydrogen Energy 42(40): 25414-25427.

74. Meziane S, AbdelhalimBentebbiche A (2019) Numerical study of blended fuel natural gas-hydrogen combustion in rich/quench/lean combustor of a micro gas turbine, International Journal of Hydrogen Energy, 44(29): 15610-15620.

75. Ophir D (1978) Ph. D Thesys, Language for Processes Of Numerical Solutions To 608 Differential Equations - Grid Language (GL) and Grid System (GS)", 1978, Department of Applied 609 Mathematics, Weizmann Institute of Science, Rehovot, Israel.

76. Milanese E (2009) Ricerca statistica di metodi estimativi: una applicazione delle componenti principali, Aestimum 1-15.

77. Morton TG (1977) Factor Analysis, Multicollinearity, and Regression Appraisal Models, The Appraisal Journal 45: 578-588.

78. Saltelli A, Ratto M, Tarantola S, Campolongo F (2005) Sensitivity Analysis for Chemical Models, Chemical Reviewers 105(7): 2811-2828.

79. Stocchero M (2012) Chemoinformatica. soluzioni e strumenti per le scienze e tecnologie biomediche Springer pp. 37-69.

80. Hirch C (2007) Numerical computation of internal & external flows: The Fundamentals of Computational Fluid Dynamics, 2nd (eds) pp. 700.

81. Arakawa A (1966) Computational design for long-term numerical integration of the equations of fluid motion: Two-dimensional incompressible flow. part I. Journal of Computational Physics 1(1): 119-143.

82. Fletcher CAJ (2003) Computational Techniques for Fluid Dynamics, Volume 2, Specific Techniques for Different Flow Categories, 2nd (eds).

83. Chung TJ (2010) Computational Fluid Dynamics. 2nd (eds) Cambridge University Press: New York, USA.

84. Ramakrishnann R, Dral PO, Rupp M, Von Lilienfeld OA (2015) Big Data Meets Quantum Chemistry Approximations: The Δ-Machine Learning Approach. Journal of Chemical Theory and Computation 11(5): 2087-2096.

85. Ferziger JH, Peric M (2002) Computational Methods for Fluid Dynamics Springer pp. 405-423.

86. Fox RO, Varma A Computational Models for Turbulent Reacting Flows, Cambridge University Press: Cambridge, UK, 2003.

87. Battistoni M (2007/2008) Dispense del Corso di Macchine, Combustibili e processi di combustione, Università degli Studi di Perugia 1-53.

88. Veríssimo AS, Rocha AMA, Costa M (2013) Experimental study on the influence of the thermal input on the reaction zone under flameless oxidation conditions. Fuel Process Technology 106: 423-428.

89. Shu, Z, Wang F, Dai, C, Jicang Si, Bo Wan et al. (2020) Characteristics of Nitric-Oxide Emissions from Traditional Flame and MILD Combustion Operating in a Laboratory-Scale Furnace. Journal of Thermal Science 29: 868-883.

90. Dean AM, Bozzelli JW (2000) Combustion Chemistry of Nitrogen, Gas phase Combustion Chemistry 125-341.

91. Novosselov I, Malte PC (2008) Development and Application of an Eight-Step Global Mechanism for CFD and CRN Simulations of Lean-Premixed Combustors, ASME Turbo Expo, GT 2007-27990, Journal of Engineering for Gas Turbines and Power 130(2): 021502.

92. Nicol DG, Malte PC, Development of Five Step Global Methane Oxidation-NO formation Mechanism for Lean Premixed Gas Turbine Combustion,

ASME 1999, Transaction of ASME 121: 272-280.

93. Magnussen BF (1989) Modeling of pollutant formation in gas turbine combustors based on the eddy dissipation concept. Proceedings of the 18th International Congress on Combustion Engines Tainjin, China.

94. Tham YF, Chen JY (2003) Recent Advancement on Automatic Generation of Simplified Mechanism, Western States Section/Combustion Institute, WSS-CI, paper 03F-49.

95. Li SC, Williams FA, Gerbert K (1999) A simplified, fundamentally based method for calculating NOx emissions in lean premixed combustors, Combustion and Flame 119(3): 367-373.

96. Hill SC, Smoot LD (2000) Modeling of nitrogen oxides formation and destruction in combustion systems. Progress in Energy and Combustion Science 26(4-6): 417-458.

97. Bozzelli JW, Dean AM (1995) O + NNH: A possible new route for NOX formation in flames. International Journal of Chemical Kinetics 27(11): 1097-1109.

98. Miller JA, Bowman CT (1989) Mechanism and modeling of nitrogen chemistry in combustion. Progress in Energy and Combustion Science 15(4): 287-338.

99. Lay TH, Bozzelli JW, Dean AM, Ritter ER (1995) Hydrogen Atom Bond Increments for Calculation of Thermodynamic Properties of Hydrocarbon Radical Species. The Journal of Physical chemistry 99 (39): 14514-14527.

100. Glarborg P, Alzueta MU, Dam-Johansen K, Miller JA (1998) Kinetic Modeling of Hydrocarbon/Nitric Oxide Interactions in a Flow Reactor. Combustion and Flame 115 (1-2): 1-27.

101. Calchetti G, Giacomazzi E, Rufoloni M, Pellegrini R (2003) Cinetica e combustione di miscele CH_4-O2, EHE 03/036 ENEA, UTS Fonti Rinnovabili e Cicli Energetici Innovativi, Sezione Impianti e Processi Energetici.

102. Wolf EE (1992) Methane conversions by Oxidative Processes: Fundamental and Engineering Aspects, Springer Science + Business Media, 1992, LLC.: New York, NY, USA.

103. Jones JM, Saddawi A, Dooley B, Mitchell EJS, Werner J, et al. (2015) Low temperature ignition of biomass. Fuel Process Technology 134: 372-377.

104. Hayhurst AN, Vince M (1980) Nitric oxide formation from N2 in flames: The importance of "prompt" NO. Progress in Energy Combustion and Science 6(1): 35 -51.

DOI: 10.32474/AOICS.2021.05.000209